ELSEVIER

Journal of Alloys and Compounds 223 (1995) 204–210

Journal of ALLOYS AND COMPOUNDS

From the transition metals to the rare earths – via the actinides

M.S.S. Brooks [a], O. Eriksson [b], B. Johansson [b]

[a] *European Commission, Joint Research Centre, Institute for Transuranium Elements, Postfach 2340, D-76125 Karlsruhe, Germany*

[b] *Condensed Matter Theory Group, Institute of Physics, University of Uppsala, Box 530, S-75121 Uppsala, Sweden*

Abstract

The calculated equations of state of the transition metals are dominated by the d-electron contribution to bonding and at the end of the 3d series the metals become magnetic. In contrast, the calculated equations of state of the rare earths are characterized by the lack of any f-electron contribution to bonding at ambient pressure and the metals are normally magnetic. Electronic structure calculations for the light actinides show that they fall naturally between the transition metals and rare earths. There is a large f-electron contribution to bonding, analogous to the d-electron contribution in the transition metals, and the light actinide metals are not magnetic. Relativistic effects upon the valence electrons are also much larger than in the transition metals and in actinide compounds, which frequently are magnetic, the composition of the magnetic moments contains features of both rare earth and transition metal magnetism.

Keywords: Transition metals; Rare earths; Actinides

1. Introduction

Viewed in terms of their conduction electrons, the rare earth metals are early 5d transition metals since the 5d shell is much less than half-filled and the 4f shell is chemically inert. The actinides are more complex. The light actinides are 5f transition metals with bonding 5f electrons whereas the heavy actinides, which have an essentially chemically inert 5f shell, are early 6d transition metals. The characteristic properties of transition metals are due to the centrifugal potential in the radial Schrödinger equation. The centrifugal potential is large near the nucleus and vanishes at large distances. Orbitals with large values of angular momentum are therefore pushed away from the nucleus. The centrifugal potential raises the energies of states with higher angular momenta compared with the energies of states with lower angular momenta. Therefore, states with large angular momentum and a given principle quantum number lie higher in energy than those of smaller angular momentum and become occupied later. Hence 3d states, for example, fill when the 4s and 4p states are already partially occupied whereas if it were not for the centrifugal term they would be core electrons before the 4s and 4p states became occupied.

The 3d and 4f states are the first d and f states in the Periodic Table and have no nodes to orthogonalize them to lower states. Their kinetic energies are therefore relatively small, and their wavefunctions and densities are relatively contracted. Since the size of a 3d atom is determined mostly by the 4s and 4p states, whose density lies further out as they have more nodes in the wavefunction, the 3d density lies mostly within the atom. However, because of the centrifugal potential, the 3d density is also pushed away from the nucleus. The spherical average of the 3d densities is therefore a shell at intermediate distance from the nucleus and the 3d density is small at the boundary of the atom. The effect of the centrifugal potential is therefore to raise the energy of what would be filled core states to somewhere close to zero energy so that the electrons can tunnel through to the free electron states outside the atom in the case of actinides or transition metals or form a localized but unfilled shell in the case of rare earths.

Much insight into transition metal band structure is provided by the LMTO method [1], where there is a very useful approximate description of narrow transition metal bands when they hybridize little with s and p bands. The unhybridized energy band eigenvalues are

SSDI 0925-8388(94)09004-1

$$E_{li}^{\bar{k}} = C_l + \Delta_l S_{li}^{\bar{k}} \quad (1)$$

where C_l, the band centre, and Δ_l, the bandwidth parameter, depend on potential, but $S_{li}^{\bar{k}}$, the structure constants, depend only on structure and are independent of the scale of the lattice. The bandwidth parameter is

$$\Delta_l = \frac{1}{2} SR_l^2(S, C_l) = \frac{1}{\mu_l S^2} \quad (2)$$

where $R_l(S, C_l)$ is the wavefunction evaluated at the atomic sphere boundary at the energy C_l. The band mass parameter is μ_l which is unity for free electrons but may become very large for narrow resonances. The bandwidth parameter, Δ_l, depends only on the size of the atomic sphere and the value of the wavefunction at the sphere boundary. It is therefore an atomic property and measures the probability of the electron reaching the boundary of the atom. The bandwidth is obtained from the second moment of the energy bands $\langle E^2 \rangle_{ll} = \int (E - C_l)^2 N_l(E) dE$ and may be written as

$$W_l = \Delta_l \langle E^2 \rangle_{ll} \quad (3)$$

where $\langle E^2 \rangle_{ll}$ is the second moment of the l diagonal structure constants, which is 28 for all fcc d bands and 45 for all fcc f bands. The calculated band mass parameters for the transition metals, rare earths and actinides are plotted in Fig. 1. The band masses increase across any series owing to contraction of the orbitals as the extra added electron is incompletely shielded by other electrons within the same shell. They also decrease down a column of the Periodic Table as additional orthogonality nodes push wavefunctions outwards. Clearly, the actinides fill the gap between the late 3d transition metals and the light rare earths.

2. Relativistic effects

The immediate effect of spin–orbit coupling on the energy bands of paramagnetic metals is to lead to distinct occupation numbers for the two spin–orbit bands with a given angular momentum, l. In the limit of vanishing spin–orbit splitting, $\Delta_{s.o.}$, the ratio of the population of the $j = l \pm 1/2$ bands becomes equal to the ratio of their degeneracies. However, in the other limit when $\Delta_{s.o.}$ is much greater than the bandwidth, W, the two j bands are split apart and the $j = l - 1/2$ band fills first. The ratio $R_2 = n_{j=l-1/2}/n_{j=l+1/2}$ changes from $2l/(2l+2)$ to infinity as the ratio $R_1 = \Delta_{s.o.}/W_l$ increases, as long as there is a total of less than $2l$ electrons of type l. Therefore, R_2 is an excellent measure of the importance of spin–orbit interaction in the ground state [2]. The ratio for d and f electrons in the actinide metals is plotted in Fig. 2 as a function of atomic number. R_2 approaches 3/4 and 2/3 in the limit $R_1 \to 0$ for f and d electrons, respectively. It is clear from Fig. 2 that there are considerable departures from this ratio for f electrons in the metals Np–Am, but not for d-electrons. The reason for this is that the preferential occupation of the $j = l - 1/2$ band is determined not by the spin–orbit splitting alone, but by the ratio R_1, which is inversely proportional to the bandwidth. Thus

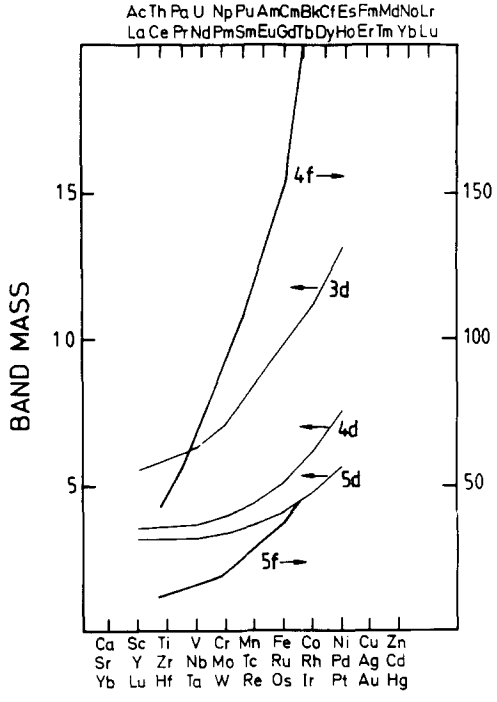

Fig. 1. Calculated band masses of the 3d, 4d and 5d transition metals, rare earths and actinides.

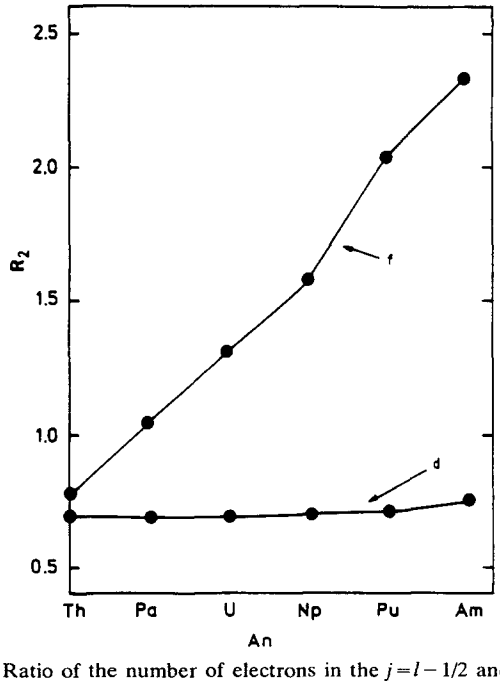

Fig. 2. Ratio of the number of electrons in the $j = l - 1/2$ and $j = l + 1/2$ bands $[l/(l+1)$ for zero spin–orbit splitting] for both d and f electrons in the actinide metals.

spin–orbit interaction does not have any major effect on the bulk ground-state properties, even for heavy metals, unless the corresponding energy bands are narrow.

Magnetic actinide compounds, even those with small lattice constants such as UN, normally have, in contrast to normal transition metals, very large orbital moments [3]. The reason is that 5f spin–orbit interaction in the actinides is far larger than the 3d spin–orbit interaction in the much lighter 3d transition metals. This is illustrated in Fig. 3, where we have plotted the spin–orbit interaction and bandwidths for the transition metals, rare earths and actinides. The bandwidths of the actinides are less than those of the 3d transition metals, whereas the spin–orbit interaction is far larger. In first order the orbital moment of an itinerant magnet is zero, but in second order the spin–orbit interaction mixes an orbital moment into the ground state. This involves mixing states from across the energy bands, and when the bandwidth is large the mixing is small and vice versa. The narrow 5f bands and the large spin–orbit interaction in actinides produce the ideal situation for itinerant electrons to support the strong orbital magnetism, which is one of the remarkable features of actinide magnetism.

3. Electronic structure of the rare earth and actinide metals

Orthogonalization to the core states increases the kinetic energy of the 5d, 6s and 6p states in rare earths and tends to exclude them from the core region. Since the core region shrinks with incomplete screening of the increased nuclear charge, the energy of the valence states decreases as the series is traversed. The opposite occurs when a given element is compressed, since the core then takes up more relative space. The effect is more pronounced for s and p states and the result is a net transfer of 5d to 6s electrons as the series is traversed. The partial s, p and d occupation numbers calculated for the di- and trivalent rare earth metals [4] are plotted as a function of atomic number in Fig. 4. The d occupation numbers decrease throughout the series for both values of valence and it is precisely the d occupation number that is correlated with the rare earth crystal structure sequence. Although the 4f states are not part of the band structure, it is the 4f electrons, through screening, that are responsible for the change in electronic structure across the series. At a constant Wigner–Seitz radius, the effect of the screening of the increased nuclear charge by the 4f electrons is isolated, and is the entire cause of any changes in conduction electron band structure. When the number of 4f electrons for a given nuclear charge is changed, as in the divalent rare earths, the effect on the conduction electron band structure is much greater. Since there is now one extra 4f electron and one less 5d electron, the 5d band becomes almost depleted by Yb.

The energy bands in actinides rise in energy under compression as in the rare earths owing to increasing kinetic energy where now the 7s states are required to be orthonormal to the 6s core states. As a function of atomic number, band filling occurs as follows. The 7s band in Fr takes the first electron, the 6d band takes most of the next three electrons between Ra and Th, the first real occupancy of itinerant 5f states occurs in Pa and thereafter the 5f band fills as far as Lr [5]. The gradual filling of the 5f bands is analogous to the filling of the d bands in transition metals, and therefore the atomic volumes of the actinides should be parabolic as a function of atomic number as first the bonding and then the anti-bonding orbitals become filled. Such

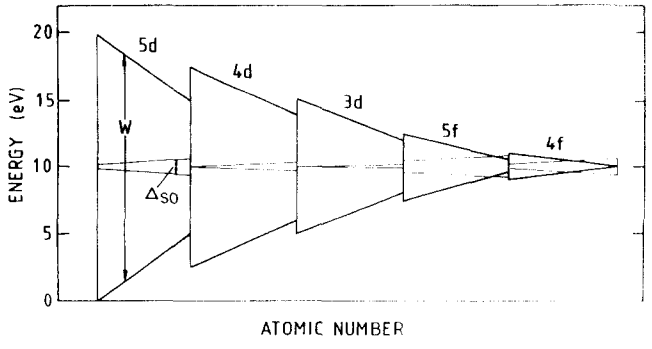

Fig. 3. Spin–orbit splitting and bandwidths of the 3d, 4d and 5d transition metals, rare earths and actinides.

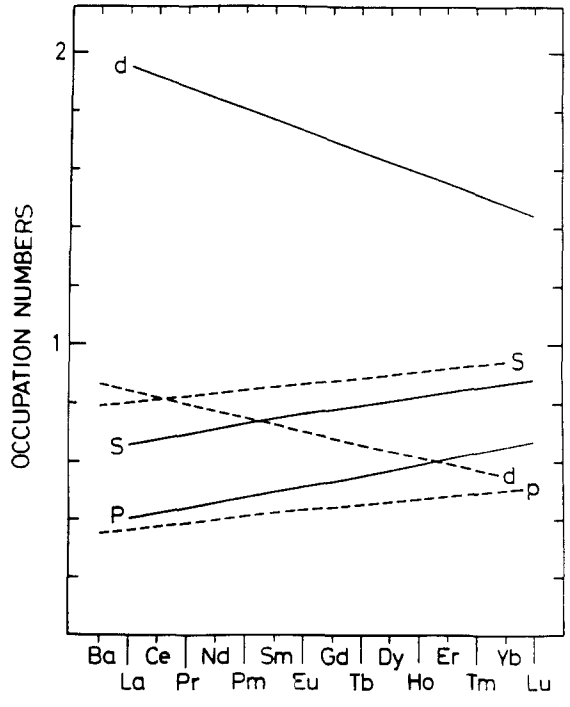

Fig. 4. Calculated s, p and d occupation numbers across the rare earth series.

a parabolic trend is indeed observed for the metals Th–Pu and the analogy with the d transition series is correct for the light actinides. However, 5f electrons are localized in the heavy actinides, where the trend in atomic volume is similar to that for the rare earths.

The 5f bandwidth decreases with increasing atomic number. This occurs because at the beginning of the series the potential due to the added proton contracts the 5f orbitals and lowers the amplitude of the wavefunction, and hence increases the band mass, at the Wigner–Seitz sphere. The narrowing is most pronounced at the beginning of the series because later the extra electron added to the system enters the 5f shell and partially screens the nuclear charge seen by the other 5f electrons. A similar trend is found for the 6d and 7s states, which are located outside the 5f shell and therefore also see the nuclear charge partially screened. For fixed atomic number, the bandwidth decreases with increasing atomic radius since the amplitude of the wavefunction at the Wigner–Seitz sphere decreases. The 5f bandwidths evaluated at the measured atomic volume remain, however, nearly constant between Th and Pu since the volume decreases, compensating for the decrease in the extension of the 5f orbital.

4. Crystal structure

For the rare earths the structure sequence hcp → Sm-type → dhcp → fcc was shown by Duthie and Pettifor [4a] to depend on the 5d occupation number, which itself is related to the Johansson–Rosengren *f*-parameter [6] used to rationalize the structure sequence. In fact, the structure sequence for the rare earths is that of early 5d transition metals and it is also found for the 4d transition metal, Y, and the heavy actinides which are 6d transition metals. Subsequent, more complete, treatment of the band structure problem for the rare earths by Skriver [4b] confirmed the essence of the Duthie–Pettifor theory at the same time adding accuracy to computed structural energy differences. By using full LMTO calculations, Skriver was also able to obtain the correct partial occupation numbers. By calculating the partial occupation numbers at the pressures needed to induce the structural transitions in La, Sm and Gd, Skriver was able to associate $n_d = 2.0$, 1.85, 1.75 with the dhcp → fcc, Sm-type → dhcp, hcp → Sm-type transitions, respectively.

The problem of the low-temperature structural stability of the light actinides is difficult since Pa is bct, U is orthorhombic with two atoms per cell, Np is orthorhombic with eight atoms per cell and Pu is monoclinic with 16 atoms per cell. Wills and Eriksson [7] have made full potential LMTO calculations for Th, Pa and U. The total energies of the three elements were calculated in three structures, fcc, bct and the orthorhombic α-U structure. The experimentally observed structures were found to have the lowest energies. Wills and Eriksson [7] argue that the preference of materials to form open structures is due to non-sphericity in the charge densities, or covalent bonding. The energy gain from covalent bonding is at the expense of the electrostatic Madelung energy. In many metals the Madelung contribution dominates and high-symmetry structures are formed. When a complex of energy bands, such as the 5f-derived bands in the actinide metals, cross the Fermi energy the covalent bonding energy gain is particularly large and low-symmetry (or open) structures become stable. Evidently, there is an analogy with the formation of Jahn–Teller or Peierls distortions in the sense that complex systems have at least one contribution to their Hamiltonian that tends to reduce the symmetry of the ground state. That charge density waves have also been observed in actinides that also have low symmetry structures [8] is suggestive that the underlying mechanism is the same. Recent calculations by Söderlind et al. [9] for transition metals at expanded volumes show that they would also have distorted structures for volumes greater than are experimentally observable.

The heavy actinide metals Am, Cm, Bk and Cf all have dhcp structures at ambient pressure and the analogy with the rare earth metals is inescapable. Eriksson et al. [4c] used the force theorem to compare the energies of the hcp and dhcp crystal structures with that of the fcc structure for the heavy actinides Am–Cf. These energies are plotted as a function of volume in Fig. 5. The dhcp structure has the lowest energy but at reduced volumes the fcc structure becomes more stable. Since a reduction in volume leads to an increase in the partial d occupation number, the fcc structure is also stable for a larger number of d electrons.

5. Cohesive energy

The cohesive energies of the transition metals [10] are not regular across the series. However, the cohesive energy, E_c, of an elemental metal is defined as the energy difference between the free atom in its ground state and the energy of the metal per atom at zero temperature and therefore contains a free atom energy contribution, ΔE_{atom}, which is the preparation energy required to take the atom from its ground state to a state similar to the non-magnetic ground-state configuration of the metal. It is this contribution which behaves irregularly across the series. The cohesive energy may therefore be written as

$$E_c = E_b - \Delta E_{atom} \quad (4)$$

thus defining the valence bond energy, E_b, which is expected to vary more smoothly across the series. If

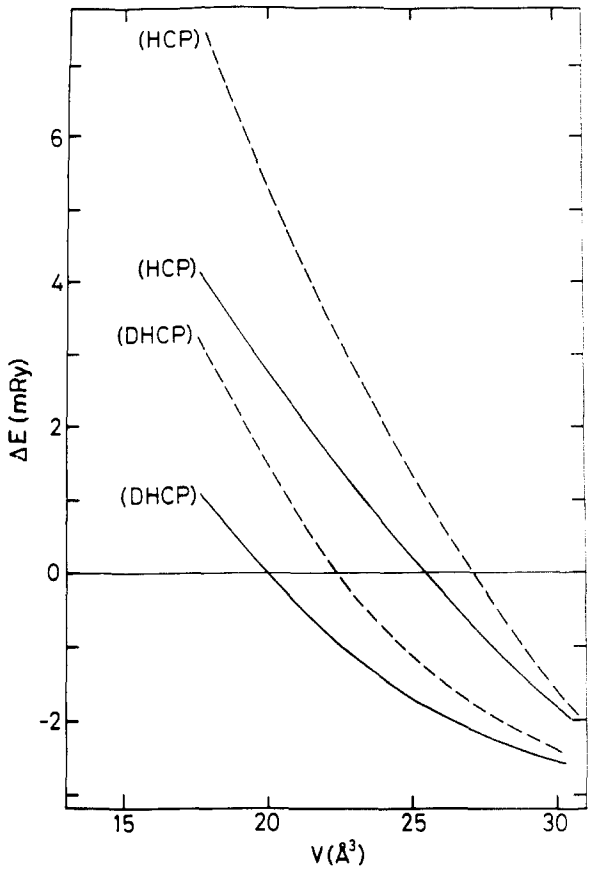

Fig. 5. Calculated energy differences for the fcc, hcp and dhcp crystal structures relative to the energy of the fcc structure (equal to zero in the graph) as a function of volume for Am (full lines) and Cf (broken lines).

the relatively small contributions to the total energy of the atom from Hund's second rule and spin–orbit interaction are neglected, ΔE_{atom} may be separated according to

$$\Delta E_{\text{atom}} = E_{\text{p}} - E_{\text{SP}}{}^{\text{LSDA}} \tag{5}$$

where E_{p} is the preparation energy required to take the atom from its ground-state configuration to the magnetic ground-state configuration of the prepared atom, which for d electrons may be taken to be the sd^{n+1} configuration. E_{p} may be obtained from experimental data. The spin polarization energy is the LSDA equivalent of Hund's first rule energy [11] and is lost when the free atom is prepared in the non-magnetic ground state.

When E_{p} and $-E_{\text{SP}}{}^{\text{LSDA}}$ are added to the measured cohesive energies shown in Fig. 6(a), the valence bond energies of the three d transition metal series shown in Fig. 6(b) are obtained. The valence bond energies, relative to the $d^{n+1}s$ non-magnetic ground states of transition metal atoms, are, in contrast to the cohesive energies, approximately parabolic functions of the d occupation number. Hence the valence bond energy is that part of the cohesive energy which is essentially a

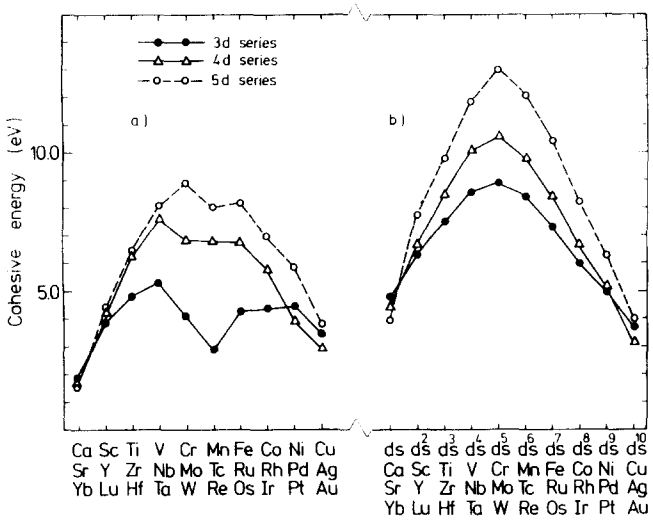

Fig. 6. (a) Measured cohesive energies of the d transition metal series; (b) calculated valence bond energies corresponding to the cohesive energies shown in (a).

solid-state property, changes smoothly across a series, and is therefore most useful for interpolation.

The cohesive energies of the trivalent rare earths should therefore be about 100 kcal mol^{-1} relative to the trivalent atomic state ($f^n ds^2$). However, the cohesive energy of gadolinium is slightly less, 95 kcal mol^{-1}, although the configuration of the free gadolinium atom is $f^7 5d6s^2$. The difference is due to the multiplet coupling between the open 4f and 5d shells in the gadolinium free atom. This coupling may easily be estimated in the local spin density approximation. In this approximation, the multiplet coupling energy is $-\frac{1}{2} J_{4f5d} \mu_{4f}{}^{S} \mu_{5d}{}^{S}$ in terms of the 4f–5d exchange interaction and the spin components of the 4f and 5d moments. We calculate J_{4f5d} to be 0.105 eV (or 2.41 kcal mol^{-1}) for a Gd atom. Therefore, with a 4f spin moment of 7 and a 5d spin moment of 1, the coupling energy is 8.4 kcal mol^{-1}.

In Gd metal, the 4f moment remains saturated but the 5d states are itinerant and have a small moment of $0.475\mu_{\text{B}}$ with a splitting of the spin up and down states at the Fermi energy due to exchange between the 4f and conduction electrons. The reduction of both the 5d moment and the 4f–5d exchange interaction means that much of the exchange energy of multiplet coupling is absent in the solid. The exchange interaction, J_{4f5d}, is reduced to 0.092 eV (2.11 kcal mol^{-1}) in Gd metal, hence the coupling is 3.5 kcal mol^{-1}. The difference between the 4f–5d multiplet coupling in the free atom and solid is therefore 8.4 − 3.5 kcal mol^{-1} or about 5 kcal mol^{-1}. The same coupling is also present in about the same magnitude in other trivalent free rare earth atoms. The cohesive energy, relative to the trivalent free atoms, should therefore be about 95 kcal mol^{-1} rather than 100 kcal mol^{-1} for metals where

there is no f shell. Similarly, the measured cohesive energy of the trivalent actinide element curium is about 90 kcal mol^{-1} [12], which may be taken to be representative of the cohesive energy of the trivalent actinide metals, again relative to the corresponding trivalent ($5f^n6d7s^2$) free atom configuration.

Eriksson et al. [4] have calculated the valence bond energies of the rare earth metals. Fig. 7(a) shows the calculated valence bond energies for trivalent La, Gd and Eu and for divalent Ba, Eu and Yb, all of which are atoms retaining the same valence in the solid as in the free atom; therefore the valence bond energies are also the cohesive energies in these cases, except for small corrections due to differences in the magnetism of the conduction electrons between free atom and solid (the calculations were not spin polarized). Also shown are the measured cohesive energies with an approximate correction made for Gd to allow for the change in the magnetism of the conduction electrons. Theory and measurement agree within a few per cent. The difference between the measured cohesive energies of the divalent and trivalent rare earths is reproduced very well. The difference between the cohesive energies of the divalent and trivalent elements is due first to the additional bonding electron in the trivalent elements, and second the d level in the trivalent atom is at a relatively high energy and a larger bonding energy is gained as the lower part of the d band is occupied. The interpolated valence bond energies for the other rare earths in Fig. 7(a) may then be used to obtain the cohesive energies.

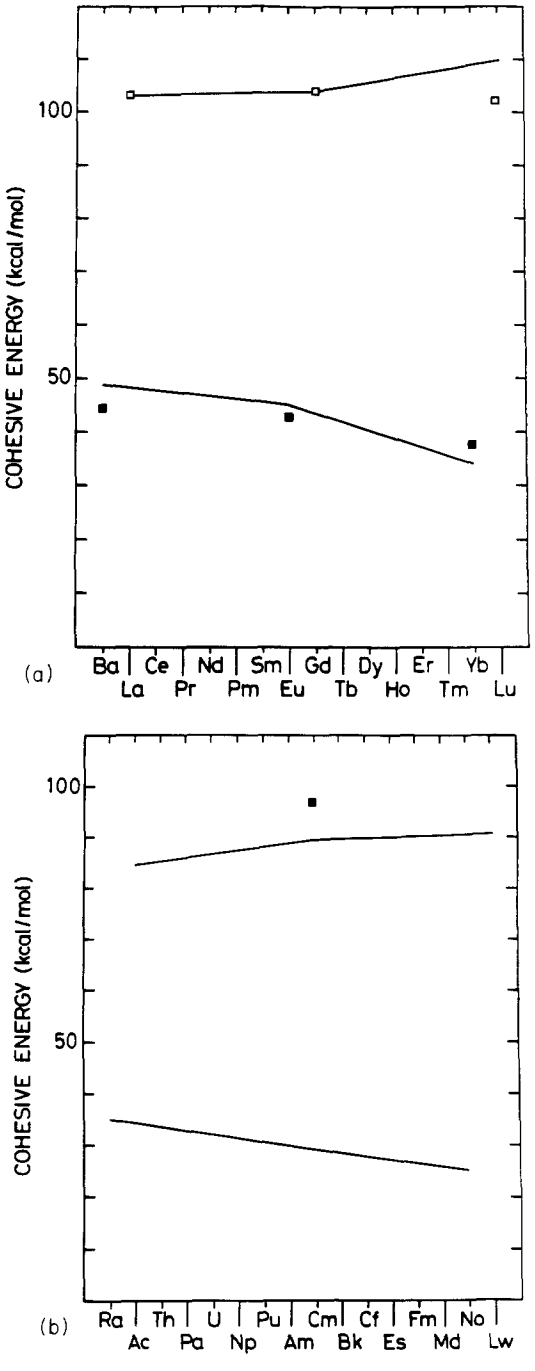

Fig. 7. (a) Calculated cohesive energies of the divalent (lower line) and trivalent (upper line) lanthanides. The measured cohesive energies are shown by squares. (b) Calculated cohesive energies of the divalent (lower line) and trivalent (upper line) actinides. The measured cohesive energy of Cm is shown by the square.

Similar cohesive energy calculations have been made by Eriksson et al. for the heavy actinides. Here the valence of the free atom ground states frequently differ from those of the rare earths. For example, the ground-state configuration of Th is d^2s^2. Further, Am metal, unlike Eu metal, is trivalent. The heavy actinides may be treated in the same way as the rare earths, however, by making the calculations for divalent Ra, Am and No, i.e., the configurations $f^{n+1}s^2$ with $n=-1$, 6, 13 and $n=0$, 7, 14 for the trivalent metals. The results are shown in Fig. 7(b). Theory is here very much on its own as the only measured cohesive energy is 92.6 kcal mol^{-1} for Cm [13], to which an estimated [14] fd coupling energy has been added. The calculated valence bond energies of both di- and trivalent heavy actinides are similar to those of the rare earths.

It has been suggested [15] that Lr, owing to relativistic effects, has an s^2p configuration in the free atom, which would modify its cohesive energy. It has also been suggested [16] that the same configuration might remain in the metal, making Lr a 3a-type metal. The calculations of Eriksson et al. [4c] reveal that Lr is a normal d transition metal. For the next element, Ku, Eriksson et al. [4c] calculated a valence bond energy of 160 kcal mol^{-1}, a value typical for a tetravalent transition metal.

The cohesive energies of the light actinides are influenced by 5f bonding. The measured cohesive energies of the light actinide metals, Pa–Am, compiled by Ward [17], are Th 6.2, Pa 5.93, U 5.52, Np 4.83, Pu 3.57 and Am 2.95 eV. Bradbury [18] reported a cohesive energy of 6.7 eV for Pa. The cohesive energy of Ac has not been measured to date. Thus the cohesive energies of the light actinides appear to decrease reg-

ularly, almost linearly, across a series, which is more reminiscent of the trend in the cohesive energies of the rare earths [19] than of a transition metal series, in apparent conflict with both measured and calculated trends in the atomic volumes. The apparent conflict is due to the free atom preparation energies, which obscure the essentially parabolic trend in the 5f band contribution to the cohesive energy [20].

The valence bond energy, relative to a trivalent and paramagnetic free atom ground state, of the light actinides in the fcc structure has been calculated by Brooks [20] and is plotted in Fig. 8. The calculated band contribution to cohesion is already falling by Pu, partly because the $5f_{5/2}$ band is more than half-filled at this stage but also because the experimental equilibrium volume, at which the energies were evaluated, is anomalously high [2]. The latter effect reduces the calculated band contribution to cohesion from the LMTO calculations even more, as here the difference between calculated and measured equilibrium volumes is even greater [5]. When a complete list of promotion and correlation energies, present in the free atoms but lost in the metal, was added to the measured cohesive energies, the valence bond energies deduced from the measured cohesive energies were found to come close to the calculated valence bond energies (Fig. 8). The added energies increase rapidly across the light actinide series. The dominant contribution is the spin-polarization energy, but the others are not negligible and it is this that is responsible for the measured decrease in the cohesive energy between Pa and Pu. The cohesive energy of actinium has never been measured but it is calculated to be 4.4 eV or about 100 kcal mol^{-1}.

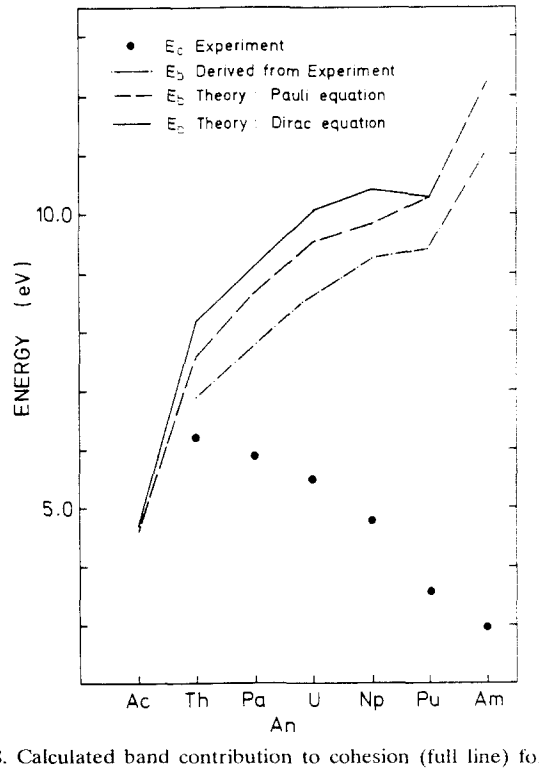

Fig. 8. Calculated band contribution to cohesion (full line) for the light actinide metals, evaluated in self-consistent RLMTO calculations. The dashed line is the same quantity evaluated in LMTO calculations. The dot-dashed line is the band contribution to cohesion evaluated from the experimental cohesive energies after analysis of the free atoms. E_c (●) are the experimental cohesive energies [17], which follow a different trend. A value of E_c for Pa of 7 eV per atom reported by Bradbury [18] is not plotted.

References

[1] O.K. Andersen, *Phys. Rev. B, 12* (1975) 3060; O.K. Andersen, O. Jepsen and D. Glötzel, in F. Bassani, F. Fumi and M.P. Tosi (eds.), *Highlights of Condensed Matter Theory. Proceedings of the International School of Physics "Enrico Fermi"*, North-Holland, Amsterdam, 1985, p. 59; H.L. Skriver, *Muffin Tin Orbitals and Electronic Structure*, Springer, Heidelberg, 1983.
[2] M.S.S. Brooks, *J. Phys. F, 13* (1983) 103.
[3] M.S.S. Brooks and P.J. Kelly, *Phys. Rev. Lett., 51* (1983) 1708.
[4] (a) J.C. Duthie and D.G. Pettifor, Phys. Rev. Lett., 38 (1977) 564; (b) H.L. Skriver, in S.P. Sinha (ed.), *Systematics and Properties of the Lanthanides*, Reidel, Dordrecht, 1983, p. 213; (c) O. Eriksson, M.S.S. Brooks and B. Johansson, *J. Less-Common Met., 158* (1990) 207.
[5] H.L. Skriver, O.K. Andersen and B. Johansson, *Phys. Rev. Lett., 41* (1978) 42.
[6] B. Johansson and A. Rosengren, *Phys. Rev. B, 11* (1975) 2835; B. Johansson and A. Rosengren, *Phys. Rev. B, 11* (1975) 1367; B. Johansson, in W.D. Corner and B.K. Tanner (eds.), *Institute of Physics Conference Series*, Vol. 37, Institute of Physics, Bristol, 1978, p. 39.
[7] J.M. Wills and O. Eriksson, *Phys. Rev.*, in press.
[8] G. Grübel, J.D. Axe, D. Gibbs, G.H. Lander, J.C. Marmeggi and T. Brückel, *Phys. Rev. B, 43* (1991) 8803; J.C. Marmeggi, G.H. Lander, S. van Smaalen, T. Brückel and C.M.E. Zeyen, *Phys. Rev. B, 42* (1990) 9365.
[9] P. Söderlind, et al., 1994.
[10] O. Gunnarsson, B.I. Lundqvist and J.W. Wilkins, *Phys. Rev. B, 10* (1974) 1319; J. Friedel and C.M. Sayers, *J. Phys. (Paris), 38* (1977) 697; M.S.S. Brooks and B. Johansson, *J. Phys. F, 13* (1983) L197.
[11] O. Gunnarsson and B.I. Lundqvist, *Phys. Rev. B, 13* (1976) 4274.
[12] J.W. Ward, R.W. Ohse and R. Reul, *J. Chem. Phys., 62* (1975) 2366.
[13] J.W. Ward, *J. Less-Common Met., 93* (1983) 279.
[14] B. Johansson and P. Munck, *J. Less-Common Met., 100* (1984) 49.
[15] L. Brewer, *J. Opt. Soc. Am., 61* (1971) 1101.
[16] D.L. Keller, *Radiochim. Acta, 37* (1984) 169.
[17] J.W. Ward, unpublished work, 1982.
[18] M.J. Bradbury, *J. Less-Common Met., 78* (1981) 207.
[19] K.A. Gschneidner, Jr., in H. Ehrenreich, F. Seitz and D. Turnbull (eds.), *Solid State Physics*, Vol. 16, Academic Press, New York, 1964, p. 276.
[20] M.S.S. Brooks, *J. Phys. F, 14* (1984) 1157.